# Application of a computational model of vagus nerve stimulation

**Article** *in* Acta Neurologica Scandinavica · February 2012

DOI: 10.1111/j.1600-0404.2012.01656.x · Source: PubMed

Acta Neurologica Scandinavica

Acta Neurol Scand DOI: 10.1111/j.1600-0404.2012.01656.x



ACTA NEUROLOGICA SCANDINAVICA

# Application of a computational model of vagus nerve stimulation

Helmers SL, Begnaud J, Cowley A, Corwin HM, Edwards JC, Holder DL, Kostov H, Larsson PG, Levisohn PM, De Menezes MS, Stefan H, Labiner DM. Application of a computational model of vagus nerve stimulation.
Acta Neurol Scand: DOI: 10.1111/j.1600-0404.2012.01656.x.


*Objectives* – The most widely used and studied neurostimulation procedure for medically refractory epilepsy is vagus nerve stimulation (VNS) Therapy. The goal of this study was to develop a computational model for improved understanding of the anatomy and neurophysiology of the vagus nerve as it pertains to the principles of electrical stimulation, aiming to provide clinicians with a systematic and rational understanding of VNS Therapy. *Materials and methods* – Computational modeling allows the study of electrical stimulation of peripheral nerves. We used finite element electric field models of the vagus nerve with VNS Therapy electrodes to calculate the voltage field for several output currents and studied the effects of two programmable parameters (output current and pulse width) on optimal fiber activation. *Results* – The mathematical models correlated well with strength–duration curves constructed from actual patient data. In addition, digital constructs of chronic versus acute implant models demonstrated that at a given pulse width and current combination, presence of a 110-$\mu$m fibrotic tissue can decrease fiber activation by 50%. Based on our findings, a range of output current settings between 0.75 and 1.75 mA with pulse width settings of 250 or 500 $\mu$s may result in optimal stimulation. *Conclusions* – The modeling illustrates how to achieve full or nearly full activation of the myelinated fibers of the vagus nerve through output current and pulse width settings. This knowledge will enable clinicians to apply these principles for optimal vagus nerve activation and proceed to adjust duty cycle and frequency to achieve effectiveness.

**S. L. Helmers[1], J. Begnaud[2], A. Cowley[3], H. M. Corwin[4], J. C. Edwards[5], D. L. Holder[6], H. Kostov[7], P. G. Larsson[8], P. M. Levisohn[9], M. S. De Menezes[10], H. Stefan[11,13], D. M. Labiner[12]**

[1]Department of Neurology, Emory University School of Medicine, Atlanta, GA USA; [2]New Products and Clinical Engineering, Cyberonics, Inc., Houston, TX USA; [3]Advanced Technology, Cyberonics, Inc., Houston, TX USA; [4]Neurology Consulting LLC, Louisville, KY USA; [5]Neurology Department, Medical University of South Carolina, Charleston, SC USA; [6]Neurology, Children's Hospital of Pittsburgh of UPMC, Pittsburgh, PA USA; [7]Department of Neurodiagnostics, Rikshospitalet University Hospital, Oslo, Norway; [8]Department of Neurodiagnostics, National Center for Epilepsy, Rikshospitalet University Hospital, Sandvika, Norway; [9]Department of Pediatrics, Children's Hospital Colorado, Aurora, CO USA; [10]Pediatric Neurology, Swedish Neuroscience Institute, Seattle, WA USA; [11]Department of Neurology, University Hospital Erlangen, Erlangen, Germany; [12]Department of Neurology, The University of Arizona, Tucson, AZ USA; [13]Interdisciplinary Epilesy Center, University Giessen-Marburg, Marburg, Germany

Key words: action potentials; electrical stimulation; epilepsy; modeling; seizures; vagus nerve

S. L. Helmers, MD, MPH, 101 Woodruff Circle, Suite 6000, Atlanta, GA 30322, USA
Tel.: +1 404 778 5943
Fax: +1 404 727 3157
e-mail: sandra.helmers@emory.edu

Accepted for publication January 24, 2012

## Introduction

The vagus nerve stimulation (VNS Therapy®; Cyberonics, Inc., Houston, TX, USA) system is an effective adjunctive treatment for medically refractory epilepsy in adults and adolescents over 12 years of age with partial onset seizures (1). A small pulse generator is surgically implanted subcutaneously in the left thoracic area and delivers intermittent electrical pulses via an electrode that is partially wrapped around the left vagus nerve in the midcervical region; the electrical signals are in turn processed in the nucleus tractus solitarius and relayed to various regions of the brain (2).

Attaining full activation of the vagus nerve requires selecting the right combination of VNS Therapy parameter settings. For optimal therapeutic effect in decreasing seizure frequency while minimizing stimulation-induced side effects, clinicians rely on attentive patient-specific titration of the five adjustable parameters: output current, frequency, pulse width, and signal ON and OFF times.

Nerve fiber activation during stimulation depends on several factors: (i) fibers located clo-

ser to the perimeter of the nerve and thereby closer to the VNS Therapy cathode are exposed to a stronger electric field and are easier to excite than fibers located deeper in the nerve, (ii) fibrous tissue encapsulation at the site of electrodes – which forms within 4–8 weeks following implantation – can increase resistance, altering the electric field and resulting in increased voltage requirements for fiber excitation (3), and (iii) fiber myelination and fiber diameter. The role of myelination and fiber diameter can be explained by briefly reviewing the properties of vagal fibers.

By systematic examination of compound action potentials, vagus nerve fibers can be classified into A, B, and C groups (4, 5). The A group (including A$\alpha$, A$\beta$, A$\gamma$, and A$\delta$) consists of myelinated, somatic, afferent, and efferent fibers with diameters ranging from 1 to 22 $\mu$m and conduction velocity ranging from 5 to 120 meters per second (m/s). The B fibers are moderately myelinated, efferent, and mainly preganglionic autonomic fibers with diameters of $\leq 3$ $\mu$m and conduction velocity ranging from 3 to 15 m/s. The myelinated A and B fibers constitute about 20% of the vagal fibers. Activation of the unmyelinated C fibers, which makes up about 80% of the vagal fibers, is not believed to be involved in the anticonvulsive effects of VNS (6).

Fibers with larger diameters require less current to reach the stimulus thresholds for recruitment and have higher conduction velocity than fibers with smaller diameters. Therefore, as current increases, fibers are recruited in the following order: A group, B group, and C group. However, successful recruitment of fibers with the same diameter varies depending upon their proximity to the stimulus source.

Maximal stimulation of the A and B fibers of the vagus nerve to achieve a therapeutic effect is the key component of treatment of seizures for several reasons:(i) As the mechanism of action for VNS Therapy is not well understood and may involve several vagal nerve tracts, selective stimulation of a group of fibers to affect only a certain portion of the brain may not be effective in many patients; (ii) at present, there is no method to measure response to vagal stimulation, making it difficult to determine which fibers are being stimulated during or after implantation of the device; and (iii) the low incidence of side effects associated with VNS Therapy suggests that maximal stimulation of the A and B fibers is well tolerated (2).

A mathematical model to understand how to achieve maximal stimulation of the A and B fibers has not been previously applied to VNS. Therefore, we developed a computational model to explore the effects of select programmable parameters. A digital model of the vagus nerve was constructed to understand the role of combinations of output current and pulse width on activation of A and B nerve fibers. Acute and chronic stimulation conditions were incorporated into the model to study the effect of tissue encapsulation at the site of electrode placement.

Output current and pulse width were studied as these parameters have an effect at the stimulation site and could be evaluated with our digital models. The effects of other parameters, such as frequency and duty cycle, are observed postsynaptically in various structures in the brain, and evaluating these parameters is beyond the scope of this article. To illustrate the nonlinear relationship between the strength (current) of an applied constant current pulse required to initiate an action potential and the duration of the pulse, strength–duration curves were used as they represent the minimum current and pulse width combinations required to activate a single nerve fiber (7, 8).

The developed modeling illustrates how to achieve full or nearly full activation of the myelinated fibers of the vagus nerve through output current and pulse width settings. This knowledge will enable clinicians to apply these principles for optimal vagus nerve activation and proceed to adjust duty cycle and frequency to achieve effectiveness.

## Materials and methods

A mathematical model consisting of three successive models was constructed to determine nerve fiber activation within the vagus nerve. First, a 3-dimensional digital representation of the geometry of the vagus nerve and VNS Therapy electrodes was created. Two different cases representing lack of connective tissue (i.e. acute implantation model) and presence of connective tissue (i.e. chronic implantation model) were also modeled. This geometry was then used in the construction of finite element models to determine the voltage distribution within the vagus nerve. Voltage distributions for several levels of output current were identified for both the acute and the chronic implant models and used in a nerve fiber model to activate individual nerve fibers within the vagus at various pulse widths. The construction of this three-part model allowed us to evaluate nerve fiber activation patterns for combinations of output current and pulse width in both the acute and the chronic implantation settings.

### Construction of the digital representation of the vagus nerve

A 3-dimensional digital representation of the vagus nerve was constructed based on measurements obtained from a histological cross-section collected from directly below the VNS Therapy electrode in a 50-year-old female who had been implanted for 3 years (W.F. Agnew, unpublished data, 1998). Notably, a 115-$\mu$m-thick layer of fibrotic tissue was found to have formed around the fiber at the area of electrode placement.

Based on data from this histological sample, the 5-cm-long digital model included nerve fibers bundled into 10 fascicles with each fascicle protected by perineurium and further bundled by the epineurium; it is referred to as the acute implant model representing the intraoperative state and very near term postoperative state following implantation. A second model of the nerve was created similar to the acute model but with the addition of a 110-$\mu$m layer of connective tissue and referred to as the chronic implant model representing the stable state reached after 4–8 weeks postimplantation (Fig. 1A). The thickness of the fibrotic tissue was based on data from the histological sample. It is acknowledged that the thickness may vary between individual patients; however, such data are not currently available.

The two digital models, each with two 2-mm-diameter VNS Therapy helical electrodes wrapped 270° around the nerve, were then used to study stimulation of the vagus nerve (Fig. 1B). In the acute implantation model, the electrodes were assumed to be in direct contact with the epineurium, and in the chronic implant model, the electrodes were assumed to be in direct contact with the connective tissue.

### Finite element analysis

Finite element analysis (ANSYS, Version 11; ANSYS, Inc., Canonsburg, PA, USA) was used to calculate the voltage distribution within the nerve during stimulation with several output current levels. The inputs required for this mathematical technique are geometry data, tissue electrical properties, and an applied stimulus. The geometry data were imported from the 3-dimensional representations of both the acute and the chronic implantation models. Additionally, tissue electrical properties for the fascicle, epineurium, perineurium, connective tissue, and surrounding tissue were taken from experimental measurements in the published literature (9–11). The applied stimulus was provided by the electrode surfaces using several output current levels. One electrode produced a positive current, and the other produced an equal, but negative current. The finite element model calculates the voltage resulting from the applied stimulus at any point within the tissue. Figure 2 shows the voltage distribution for a 2.25-mA output current pulse.

### Nerve fiber activation model

Another computational model was constructed to predict the response of a nerve fiber when voltage is applied to the surrounding tissue. The values for conductances and capacitances needed for this model were established in previous work (12–15). The voltage in the tissue surrounding each nerve fiber was imported from the finite element models. This voltage was applied for a time equal to several pulse widths. At each of 90 locations within the vagus nerve, several 2-cm-long nerve fibers with diameters varying between 1 and 10 $\mu$m were tested to determine the smallest diameter fiber activated. The model assumes constant transmembrane conductances until a threshold potential is reached.

### Construction of strength–duration curves

To correlate the findings from the model to actual patient data, strength–duration curves

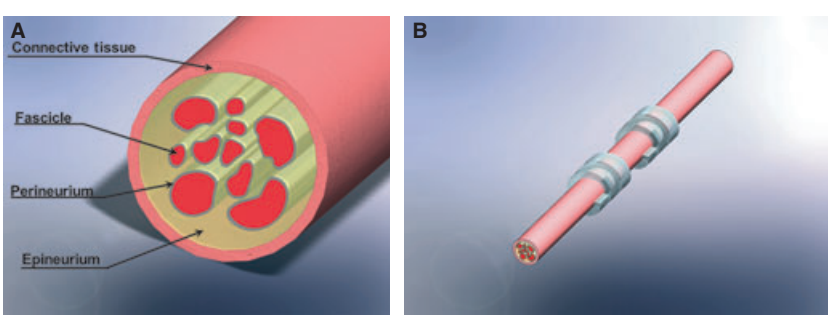


**Figure 1.** (A) A cross-sectional representation of the mathematical model of the vagus nerve showing 10 nerve fascicles of varying sizes surrounded by perineurium and epineurium, enclosed by fibrotic connective tissue. (B) A digital model with two 2-mm-diameter vagus nerve stimulation Therapy helical electrodes wrapped 270° around the nerve.

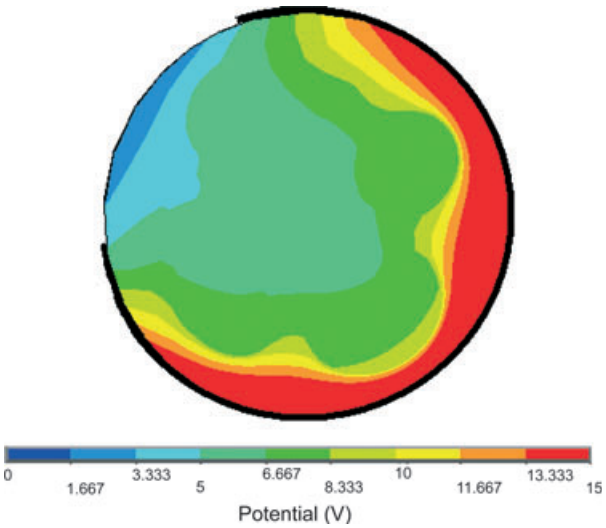


**Figure 2.** The solution to the ANSYS finite element model, showing voltage field distribution for a 2.25 mA current. This figure represents a cross-section taken from beneath the anode of the modeled nerve. Because fiber recruitment cannot be determined from voltage field data alone, these data were used in the linear nerve fiber model. The scale under the model shows the colors that correspond to various levels of voltage. The black line partially encircling the nerve represents the electrode ribbon. As the distance from an electrode increases, the voltage decreases.

were constructed; such curves illustrate the nonlinear relationship between pulse width and output current; and as the pulse width of a given stimulus decreases, the threshold current must increase to compensate (7).

As measurements of chronic compound action potentials are currently not possible with the device, a reasonable approach was used to estimate the rheobase current from available patient data for responders in the VNS Therapy Epilepsy Patient Outcome Registry (data on file, Cyberonics, Inc.) and the E05 VNS Therapy extension study (16). Responders are defined as patients (aged $\geq 12$ years) who experienced $\geq 50\%$ reduction in seizure frequency at 12 months following implantation with at least a 5% duty cycle (i.e. 30-s signal ON and 10-min signal OFF times) and at 10-Hz signal frequency or higher. It should be noted that duty cycle is defined as a percentage of stimulation time:

$$\text{Duty cycle} = \text{ON time} + 4\,\text{s}/\text{ON time} + \text{OFF time}$$

Settings of 1.5 mA with either 250 or 500 $\mu$s pulse width appeared to be the most widely used parameter combination in responders regardless of variable signal frequencies and duty cycles. Using these parameters (1.5 mA and 500 $\mu$s), the Lapicque equation was solved and fitted to the rest of the strength–duration curves (at a rheobase current of 1.48 mA and varying pulse widths, such as 130, 250, 750, and 1000 $\mu$s).

In the Lapicque equation, $I_{th}$ is the threshold current, $I_{rh}$ is the rheobase current, W is the pulse width (i.e. duration), and $\tau_m$ is the nerve fiber membrane time constant (7):

$$I_{th} = \frac{I_{rh}}{1 - \exp(W/\tau_m)}$$

Data collected by Evans et al. (17) from intraoperative measurements of compound action potentials of A fibers in implanted patients were also used; the authors set the pulse width at 130 $\mu$s, and the output current was increased up to 1 mA until the maximum compound action potential was observed.

## Results

### Parameter settings for maximum vagus nerve activation

Using the mathematical models, the effects of the combination of two adjustable parameters (output current and pulse width) on activation of nerve fibers were studied. It should be noted that according to experimental measurements from Schnitzlein et al. (18), the myelinated fibers in the left cervical vagus are composed of 4% fibers with a diameter larger than 10 $\mu$m, 13% with a diameter between 3 and 9 $\mu$m, and 83% with a diameter below 3 $\mu$m. Assuming a uniform distribution of fiber diameters across each class, 100% of A and B fibers have a diameter >1 $\mu$m, 58% with a diameter larger than 2 $\mu$m, 17% with a diameter larger than 3 $\mu$m, and 12% with a diameter larger than 5 $\mu$m. If the results from the models are weighted with these values, the percentage of nerve fibers activated can be determined for the entire nerve for each output current and pulse width combination.

The effect of various pulse widths ranging from 130 to 750 $\mu$s was tested in the acute and chronic implant models, and when fiber activation between 130- and 250-$\mu$s pulse widths at equal output currents was compared, it was noted that activation is reduced by about 3% at 130 $\mu$s. There was a 0.7% increase in activation when comparing equal output currents at 250 and 500 $\mu$s, and there was no difference in activation between equal output currents at 500 and 750 $\mu$s. Therefore, we proceeded to utilize the 500-$\mu$s pulse width in studying the effects of variable current and fibrosis on fiber activation.

The first two panels in Fig. 3 represent the effect of different output currents on the chronic implant model. The connective tissue considered to be present in and around the electrode alters the electric field of the model, and as the output current increases from 0.75 to 1.5 mA (at a constant pulse width of 500 $\mu$s), smaller fibers are recruited (shown as increased numbers of yellow and red dots); overall, 20% more nerve fibers were activated when the current was increased from 0.75 to 1.5 mA. It should be noted that the electrode is depicted as a blue circular line in Fig. 3; the electrode does not fully encircle the vagus nerve but wraps approximately 270° around it.

The mathematical working models were also used to compare the effect of fibrosis on fiber activation (Fig. 3). In the acute implant model, a current of 1.5 mA with 500-$\mu$s pulse width stimulated all fibers with a diameter >1 $\mu$m (depicted as red dots in Fig. 3); that is, an estimated 99.5% of A and B fibers were activated. However, at the same current and pulse width, the presence of the fibrotic tissue increased the resistance of the chronic implant model, and limited number of fibers were stimulated; mainly fibers with diameters <3 $\mu$m and overall an estimated 53% of fibers were activated. The model assists in elucidating the effect of fibrosis on activation of the different fiber diameters.

### Strength–duration curve for VNS therapy responders

Derived strength–duration curves are presented in Fig. 4. The top curved line was fitted based on data from responders in the VNS Therapy Registry and the E05 extension study. The middle curved line was constructed based on data collected by Evans et al. (17); it should be noted that because the study was conducted intraoperatively, the results may not represent the stimulation needed to recruit fibers as fibrosis develops.

The top and middle curved lines follow the trend that smaller pulse widths require a higher current to elicit a full activation response and likewise the activation threshold plateaus after approximately 250-$\mu$s pulse width. Utilizing the data from the patient registry and E05 extension study, we found that 57.5% of responders had settings within the zone between 0.75 and 1.5 mA at 250 to 500 $\mu$s (purple line; maximum target) and 36.2% of responders were programmed within the same pulse width range but with output currents >1.5 mA (orange line; minimum target). We identified very few responders below an output current of 0.75 mA (green line).

These data suggest a range for target output current and pulse width to ensure activation of most of the A and B fibers within the nerve, and we tested the range with our model. Figure 4 shows each of these strength–duration curves and the target zone (between minimum and maximum lines) that may increase the likelihood of a therapeutic response. The mathematical models correlated well with the strength–duration curves. In the chronic cases, parameter combinations at and above the maximum target line showed that the majority of the fibers in the vagus (>50%) had been activated. The acute models showed >50% fiber activation at combinations at and above the minimum target line. Furthermore, all models showed a negligible

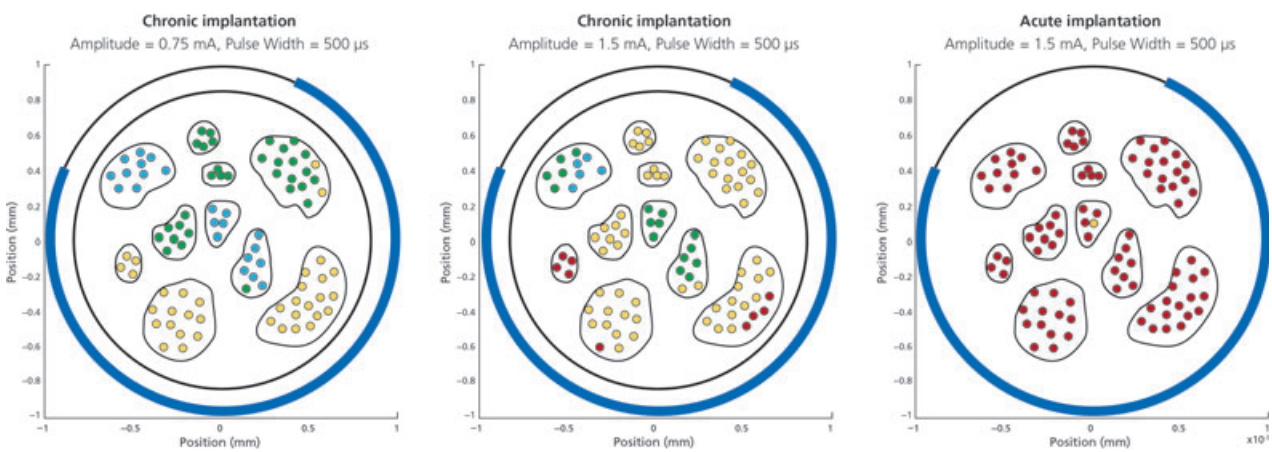


**Figure 3.** Comparison of fiber activation in 'chronic' implant model of vagus nerve at 0.75 and 1.5 mA output currents and 'acute' implant model at 1.5 mA output current at 90 locations. All pulse widths are equal (500 $\mu$s). Red dots: All fibers with diameters >1 $\mu$m are stimulated, that is, at that location, all A and B fibers would be stimulated. Yellow dots: All fibers with diameter >2 $\mu$m are stimulated (i.e. 58% of A and B vagus fibers). Green dots: All fibers with diameter >3 $\mu$m are stimulated (i.e. 17% of vagus fibers). Cyan dots: All fibers with diameter >5 $\mu$m are stimulated (i.e. 12% of vagus fibers). The blue line represents the position of the vagus nerve stimulation Therapy-stimulating electrode.

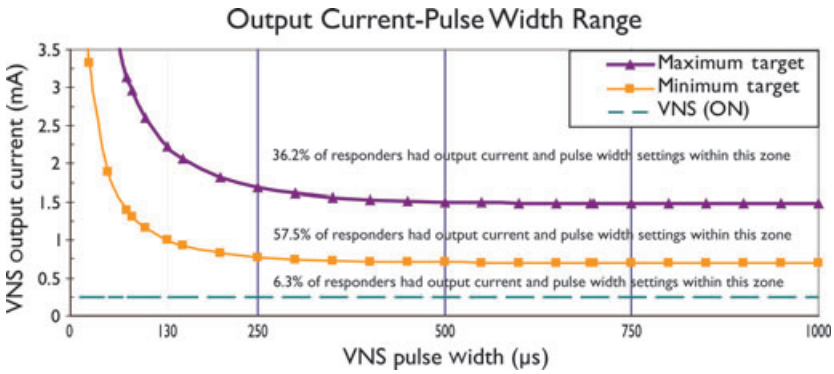


**Figure 4.** Vagus nerve stimulation threshold strength–duration curve. The 'minimum target' curve represents the minimum output current pulse width needed to activate the nerve completely in the absence of tissue ingrowth. An increase in resistance because of tissue ingrowth may occur during the first several weeks after surgery. This increase may require additional stimulation per pulse for adequate recruitment of the vagal afferents. Very few patients (6.3%) responded with output current and pulse width falling below the 'minimum target' line. More than half of the responders (57.5%) had output current pulse width combinations above the 'minimum target' line and below the 'maximum target' line; 36.2% of responders had output current pulse width combinations above the maximum target line.

increase in fiber activation when the pulse width was increased beyond 500 $\mu$s.

To summarize, choosing a combination of output current pulse width parameters lying between the minimum and maximum target lines increases the likelihood of maximizing the compound action potential, given the factors involved (fiber type and composition, fiber location, and fibrosis).

Recent studies of strength–duration relationships using animal models presented results similar to our findings in dogs (19), but not in rats (20). The variable findings may be attributed to differences in vagus nerve anatomy as well as differences in measurement techniques.

## Discussion

Attaining full activation of the vagus nerve requires selecting the right combination of VNS Therapy parameter settings. We used computer modeling to define effective activation of the vagus nerve at various output currents and pulse widths. The combination of these two parameter settings defines the amount of charge delivered to the nerve fibers and reflects the probability of achieving effective activation of the vagus nerve. Based on the computer model, we found that for optimal stimulation, output current settings may range between 0.75 and 1.75 mA with pulse width settings of 250 or 500 $\mu$s. Such settings will likely provide sufficient vagal activation in adults and in children over 12 years of age, with minimal side effects. Notably, these settings may not apply to children under the age of 12 years, as Koo et al. (21) demonstrated intraoperatively that children 10 years and younger require higher output currents to achieve activation of the vagus which may be due to level of nerve maturation during development.

### Optimizing battery life

To understand the effects of different combinations of output current and pulse width on battery life, we calculated charge as a product of output current and pulse width from the datapoints on the maximum target line shown in Fig. 4. A 1.5 mA output current is high enough to reach the maximum target zone at a pulse width of 500 $\mu$s, and varying the pulse widths to 750 or 1000 $\mu$s does not change the nerve activation level (Fig. 4). However, with longer pulse widths, the calculated charge per pulse increases from 0.7 $\mu$C (at 500 $\mu$s) to 1.1 and 1.5 $\mu$C (at 750 and 1000 $\mu$s, respectively) (Fig. 5). At pulse widths of 130 and 250 $\mu$s, higher threshold output currents (2.25 and 1.75 mA, respectively) are required for effective activation of the nerve and yet produce the lowest charge per pulse (0.437 and 0.292 $\mu$C, respectively) for effective activation of the nerve. Because battery life is correlated with charge, the lower pulse widths (250 and 130 $\mu$s) and their respective threshold currents conserve battery life more effectively than the longer pulse widths (500, 750, or 1000 $\mu$s). It can be extrapolated that the maximum target line shown in Fig. 4 provides appropriate guidelines to utilize during upward titration of the output current in implanted patients during the initial titration period, and for optimal activation of the nerve fibers while conserving battery life, pulse width settings beyond 500 $\mu$s are not needed.

Battery demand is also affected by duty cycle and signal frequency (increases in both of these

parameters will negatively affect battery longevity), but such considerations are beyond the scope of this article.

### Future refinement of the computer model

The computer model was developed according to specific assumptions. In the future, this computer model can be further refined to include additional factors that may influence the effectiveness of VNS Therapy (e.g. signal frequency, duty cycle, virtual anodes, virtual cathodes, conduction blocking, and fibrotic tissue of varying thickness). At present, the contribution of signal frequency (most common settings are 20 or 30 Hz) is not fully understood. Similarly, the effects of adjusting the duty cycle are not fully understood. Duty cycles describe the percentage of the stimulation period to stimulation-free period. Several algorithms have been developed that combine periods of increasing output current and pulse width followed by longer periods of increasing duty cycle (22). It should be noted that duty cycles >50% in combination with signal frequencies $\geq$50 Hz are not recommended owing to possible neural degeneration noted in animal studies (23).

As mentioned earlier, the electrode does not fully encircle the vagus nerve but wraps approximately 270° around it. This partial positioning of the electrode contributes to potential 'quiet spots' where higher stimulation may be required for the activation of the nerve fibers and may be a contributing factor in patient response to the device. However, we are unable to make a recommendation on the positioning of the electrodes, as no method has been developed to predict whether a particular fascicle or multiple fascicles within the nerve should be recruited to elicit a therapeutic response.

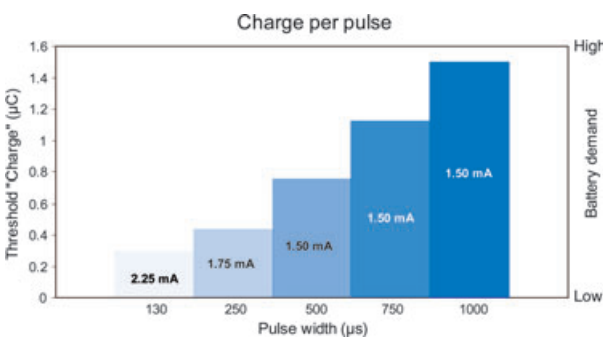


**Figure 5.** The amount of charge for various pulse width and output current combinations based on the 'maximum target' line shown in Fig. 4. Each of the combinations of pulse width and output current has similar clinical effectiveness; however, some of the combinations deliver higher charges and will result in decreased battery life.

Despite these limitations, this study has – for the first time – enabled clinicians to envision the changes in output current and pulse width as they affect the activation of the vagus nerve. This knowledge will enable clinicians to apply these principles for optimal vagus nerve activation and possibly improve the treatment of patients.

## Acknowledgements

Cyberonics, Inc. – manufacturer of the VNS Therapy® – sponsored a series of roundtable discussions in conjunction with the annual American Epilepsy Society meetings beginning in 2008. Medical writing assistance was provided by MaryAnn Foote, PhD, and Karishma Manzur, PhD, and was compensated by Cyberonics, Inc. Susan E. Siefert, ELS, CBC, an employee and stockholder of Cyberonics, Inc., provided editorial services.

## Conflict of Interest and Sources of Funding Statement

Mr. Begnaud and Mr. Cowley are employees and stockholders of Cyberonics, Inc. The other authors received a modest honorarium, but no travel assistance, from Cyberonics, Inc., for their participation in the roundtable discussions. Dr. Helmers has received consulting fees from Cyberonics, Inc., and UCB. Dr. Corwin has received honoraria for advisory board participation and/or speaker honoraria from Cyberonics, Inc, GlaxoSmithKline, Novartis Corporation, Ortho-McNeil, Pfizer Inc., and UCB. Dr. Edwards has received speaker honoraria from Cyberonics, Inc., GlaxoSmithKline, and UCB and has received consulting fees from Cyberonics, Inc. Dr. Holder has received speaker honoraria from Cyberonics, Inc. Dr. Larsson has received consulting fees from Cyberonics, Inc. Dr. Stefan has received honoraria for advisory board participation from Cyberonics, Inc., and Medtronic, Inc., and has received speaker honoraria from Eisai Co. Ltd., GlaxoSmithKline, Janssen-Cilag, Pfizer Inc., and UCB S.A. Dr. Labiner has received consulting fees, speaker honoraria, and research grants from Cyberonics, Inc., and has received support from Eisai Co. Ltd., GlaxoSmithKline, Ortho-McNeil, Pfizer Inc., UCB, and the Centers for Disease Control and Prevention. Drs. Kostov, Levisohn, and De Menezes state that they have not received any additional funding relevant to the content of this article.

## References

1. Elliott RE, Morsi A, Kalhorn SP et al. Vagus nerve stimulation in 436 consecutive patients with treatment-resistant epilepsy: long-term outcomes and predictors of response. Epilepsy Behav 2011;**20**:57–63.
2. Schachter SC, Schmidt D. Vagus nerve stimulation. London, UK: Martin Dunitz, 2001.
3. Grill WM, Mortimer JT. Electrical properties of implant encapsulation tissue. Ann Biomed Eng 1994;**22**: 23–33.
4. Gasser HS, Grundfest H. Axon diameters in relation to the spike dimensions and the conduction velocity in mammalian A fibers. Am J Physiol 1939;**127**:393–414.
5. Ruch TC, Patton HD. Physiology and biophysics. Philadelphia, PA: WB Saunders, 1965.

6. Krahl SE, Senanayake SS, Handforth A. Destruction of peripheral C-fibers does not alter subsequent vagus nerve stimulation-induced seizure suppression in rats. Epilepsia 2001;**42**:586–9.
7. Merrill DR, Bikson M, Jefferys JG. Electrical stimulation of excitable tissue: design of efficacious and safe protocols. J Neurosci Methods 2005;**141**:171–98.
8. Smith CD, Geddes LA, Bourland JD et al. The chronaxie and propagation velocity of canine cervical vagus nerve fibers in vivo. Cardiovasc Eng 2001;**1**:77–84.
9. Veltink PH, van Veen BK, Struijk JJ et al. A modeling study of nerve fascicle stimulation. IEEE Trans Biomed Eng 1989;**36**:683–92.
10. Goodall EV, Kosterman LM, Holsheimer J et al. Modeling study of activation and propagation delays during stimulation of peripheral nerve fibers with a tripolar cuff electrode. IEEE Trans Rehabil Eng 1995;**3**:272–82.
11. Frieswijk TA, Smit JP, Rutten WL et al. Force-current relationships in intraneural stimulation: role of extraneural medium and motor fibre clustering. Med Biol Eng Comput 1998;**36**:422–30.
12. Dodge FA, Frankenhaeuser B. Sodium currents in the myelinated nerve fibre of *Xenopus laevis* investigated with the voltage clamp technique. J Physiol 1959;**148**:188–200.
13. Frankenhaeuser B, Huxley AF. The action potential in the myelinated nerve fiber of *Xenopus laevis* as computed on the basis of voltage clamp data. J Physiol 1964;**171**:302–15.
14. Goldman L, Albus JS. Computation of impulse conduction in myelinated fibers; theoretical basis of the velocity-diameter relation. Biophys J 1968;**8**:596–607.
15. Warman EN, Grill WM, Durand D. Modeling the effects of electric fields on nerve fibers: determination of excitation thresholds. IEEE Trans Biomed Eng 1992;**39**:1244–54.
16. Morris GL 3rd, Mueller WM. Long-term treatment with vagus nerve stimulation in patients with refractory epilepsy. The Vagus Nerve Stimulation Study Group E01-E05. Neurology 1999;**53**:1731–5.
17. Evans MS, Verma-Ahuja S, Naritoku DK et al. Intraoperative human vagus nerve compound action potentials. Acta Neurol Scand 2004;**110**:232–8.
18. Schnitzlein HN, Rowe LC, Hoffman HH. The myelinated component of the vagus nerves in man. Anat Rec 1958;**131**:649–67.
19. Castoro MA, Yoo PB, Hincapie JG et al. Excitation properties of the right cervical vagus nerve in adult dogs. Exp Neurol 2011;**227**:62–8.
20. El Tahry R, Mollet L, Raedt R et al. Repeated assessment of larynx compound muscle action potentials using a self-sizing cuff electrode around the vagus nerve in experimental rats. J Neurosci Methods 2011;**198**:287–93.
21. Koo B, Ham SD, Sood S et al. Human vagus nerve electrophysiology: a guide to vagus nerve stimulation parameters. J Clin Neurophysiol 2001;**18**:429–33.
22. Heck C, Helmers SL, DeGiorgio CM. Vagus nerve stimulation therapy, epilepsy, and device parameters: scientific basis and recommendations for use. Neurology 2002;**59**:S31–7.
23. Agnew WF, McCreery DB, Yuen TG et al. Histologic and physiologic evaluation of electrically stimulated peripheral nerve: considerations for the selection of parameters. Ann Biomed Eng 1989;**17**:39–60.